Measurement of thermal accommodation coefficients using laser-induced incandescence
Daun, K. J.; Mercier, P. H.; Smallwood, G. J.; Liu, F.; Le Page, Y.

Publisher's version / Version de l'éditeur:

2007 ASME-JSME Thermal Engineering Summer Heat Transfer Conference [Proceedings], 2007

WR001844 *CT-07781237-4*

WR001844 **CISTI ICIST** CT-07781237-4

Document Delivery Service
in partnership with the **Canadian Agriculture Library**

Service de fourniture de Documents
en collaboration avec **la Bibliothèque canadienne de l'agriculture**

THIS IS NOT AN INVOICE / CECI N'EST PAS UNE FACTURE

MARIA CLANCY
DGO
INST FOR CHEM PROCESS & ENVIR TECH
NATIONAL RESEARCH COUNCIL CANADA
M-12, ROOM 141, 1200 MONTREAL RD.
OTTAWA, ON K1A 0R6
CANADA

ORDER NUMBER:	**CT-07781237-4**
Account Number:	WR001844
Delivery Mode:	XLB
Delivery Address:	
Submitted:	2009/03/03 13:13:53
Received:	2009/03/03 13:13:53
Printed:	2009/03/03 14:04:09

Extended **Periodical** **Fax - transcribed** **CANADA**

Client Number:	MARIA CLANCY MAR 02 2009 # 7
Author:	DAUN K J; MERCIER PH; SMALLWOOD G J, ET AL
Date:	2007
Article Title:	MEASUREMENT OF THERMAL ACCOMODATION COEFFICIENTS USING LASER....
Series Title:	ASME-JSME THERMAL ENGINEERING CONFERENCE AND SUMMER HEAT TRANSFER CONFERENCE, VANCOUVER, BC, JULY 8-12, 2007

INSTRUCTIONS: ********ATTN: MARIA CLANCY********

Estimated cost for this 7 page document: $0 document supply fee + $0 copyright = $0

Proceedings of HT2007
2007 ASME-JSME Thermal Engineering Summer Heat Transfer Conference
July 8-12, 2007, Vancouver, British Columbia, CANADA

HT2007-32104

MEASUREMENT OF THERMAL ACCOMMODATION COEFFICIENTS USING LASER-INDUCED INCANDESCENCE

K. J. Daun, P. H. Mercier, G. J. Smallwood, F. Liu, and Y. Le Page
Institute for Chemical Process and Environmental Technology
National Research Council of Canada

ABSTRACT

Laser-induced incandescence (LII) is used to measure the thermal accommodation coefficient between soot sampled from a well-characterized flame and various monatomic and polyatomic gases. These measurements show that the thermal accommodation coefficient between soot and monatomic gases increases with molecular mass due to the decreasing speed of incident gas molecules and corresponding decrease in surface deformation rate, and that energy is transferred preferentially from the surface to the translational mode of the polyatomic gas molecules over internal energy modes.

INTRODUCTION

The thermal accommodation coefficient, α_T, defines the energy transfer efficiency when an incident gas molecule is scattered by a thermally-vibrating surface. Knudsen [1] was the first to formally define the this parameter as

$$\alpha_T = \frac{T_{g,o} - T_g}{T_s - T_g}, \qquad (1)$$

where T_s is the surface temperature and T_g and $T_{g,o}$ are the kinetic temperatures of incident and scattered gas molecular streams, respectively. Since these temperatures correspond to the energies of the surface and gas states, an equivalent definition of the thermal accommodation coefficient is

$$\alpha_T = \frac{E_{g,o} - E_g}{E_s - E_g}, \qquad (2)$$

where E_s, E_g and $E_{g,o}$ correspond to the temperatures in Eq. (1).

Recent interest in thermal accommodation coefficients has been driven largely by time-resolved laser-induced incandescence (LII), a diagnostic technique for measuring the particle size distribution in refractory aerosols. In this procedure, a nanosecond laser pulse energizes the aerosol particles in the laser path to incandescent temperatures, typically 3000-3600 K in low fluence experiments, and the resulting spectral incandescence is then measured as the particles cool back to the ambient gas temperature. Since larger particles cool slower than smaller particles, the particle size distribution can be inferred from the observed incandescence decay [2]. When carrying out this measurement, however, it is crucial to accurately model the heat transfer from the aerosol particles to the gas, which occurs primarily by conduction in the free-molecular regime and is thus a strong function of α_T. Knowledge and understanding of the thermal accommodation coefficient is thus paramount when doing particle sizing through time-resolved LII.

On the other hand, if the particle size distribution is measured independently, the thermal accommodation coefficient can be determined from the observed incandescence decay rate. In principle this is an excellent way of measuring α_T since adsorbed contaminants on the particle surface, which confound other types of experimental techniques [3-4], are promptly removed by the laser pulse. Several recent studies [5-9] have endeavored to use time-resolved LII to measure thermal accommodation coefficients for different gas-particle systems, with the objective of using the recovered value to perform aerosol particle sizing. Most of these experiments measure α_T between soot and the surrounding gas in a flame [5, 8] or between carbon black and air [7], although Starke et al. [6] and Eremin et al. [9] measured α_T for He/C, Ar/C, CO/C, C_3O_2/C, and Ar/$Fe(CO)_3$ using shock tubes. Unfortunately, these studies have revealed little about the true physics of gas-surface scattering in time-resolved LII experiments, and in some cases have actually confounded the understanding of α_T by reporting erroneous results [10]. The prevailing uncertainty in the value and physical nature of α_T must first be resolved in order for LII to mature into a reliable tool for aerosol particle sizing [11].

The objective of this paper is to elucidate the fundamental physics of gas/surface molecular interactions that occur in time-resolved LII, in particular the dependence of α_T on the molecular mass and the structure of the gas molecule, by examining LII-measured thermal accommodation coefficients between soot extracted from a well-characterized laminar diffusion flame and various gases. We first demonstrate the dependence of the thermal accommodation coefficient on the molecular mass of the gas by analyzing experimentally-measured α_T values for soot in monatomic gases and corresponding results of a molecular dynamics study. Secondly, a comparison of α_T values for soot entrained in monatomic gases with results of soot in polyatomic gases shows that polyatomic gas molecules accommodate energy preferentially into their translational state, instead of their vibrational and rotational states. This knowledge provides a foundation on which to develop more accurate heat transfer models and improve the reliability of aerosol particle sizing through time-resolved LII analysis.

NOMENCLATURE

A_{cond}	Effective heat transfer area, m^2
$c(T_g)$	Mean incident molecular speed, ms^{-1}
c_s	Soot specific heat, $Jkg^{-1}K^{-1}$
d_p	Primary particle dimameter, m
E	Energy advected by a molecular stream, J
E_s	Modulus of elasticity, Pa
e	Coefficient of restitution
k_B	Boltzmann's constant, 1.380×10^{-23} $J\cdot molecule^{-1}\cdot K^{-1}$
m_g	Gas molecular mass
m_s	Surface atomic mass
N_p	Number of primary particles per aggregate
P_g	Gas pressure, Pa
q_{cond}	Conduction heat transfer rate, W
t	Time, s
$T_p(t)$	Particle temperature, K
T_g	Gas temperature, K
$u_{g,i}$	Incident gas molecular velocity, ms^{-1}
$u_{g,o}$	Recoil gas molecular velocity, ms^{-1}
$u_{g,i}^*$	Reduced velocity, $u_{g,i}/V_s$
V_s	Effective surface velocity, ms^{-1}
α_T	Thermal accommodation coefficient
γ	Specific heat ratio
Λ	Fraction of incident kinetic energy transformed to deformation work
λ	Wavelength, nm
μ	Mass ratio, m_g/m_s
ν_s	Poisson's ratio
ρ_g	Effective gas molecular density, $kg\ m^{-3}$
ρ_s	Soot density, $kg\ m^{-3}$
$\theta(t)$	$T_p(t)-T_g$
ζ_{int}	Number of internal degrees of freedom

Subscripts and Superscripts

i	Incident molecular stream
int	Internal degrees of freedom/energy
o	Outgoing molecular stream
$trans$	Translational energy

EXPERIMENTAL MEASUREMENT TECHNIQUE

The experimental apparatus is shown schematically in Fig. 1, and consists of a laminar diffusion flame, soot sampling system, and LII chamber. The ethylene laminar diffusion flame is generated with a coflow burner operating under conditions described in [8]. The sampling system consists of a venturi mini-eductor with a 0.030 inch critical diameter and a soot sampling probe connected to the venturi throat. Motive gas flows through the venturi at 20 liters per minute, causing a pressure drop at the venturi throat that pulls soot from the flame centerline at a height of 52 mm above the burner into the motive gas stream. Although gas from the flame and the surroundings is also entrained into the sampling system, a large dilution ratio ensures that it has a negligible influence on the experimental results. The motive gas and soot then enter the LII chamber, where the soot particles are energized with a pulsed ND:YAG laser operating 16 mJ per pulse at 20 Hz and 1024 nm. The laser heats the soot to a peak temperature of approximately 3600 K, and the resulting incandescence is imaged onto two photomultipliers equipped with narrow-band interference filters centered at 397 nm (36 nm FWHM) and 782 nm (19 nm FWHM), respectively. Transient signals from the photomultipliers are digitized and averaged over 100 shots to mitigate shot noise resulting in a set of incandescence decay curves and a pyrometrically-defined temperature decay curve as shown in Fig. 2.

The LII data is analyzed following the procedure described in [8]. After the laser pulse, the soot cooling rate is governed by

$$\rho_s c_s N_p \frac{\pi d_p^3}{6}\frac{dT_p}{dt} = -q_{cond}\left[T_p(t)-T_g\right], \tag{3}$$

where ρ_s and c_s are the density and specific heat of soot, N_p is the number of primary particles per soot aggregate, d_p is the primary particle diameter, and q_{cond} is the net heat transfer from the aggregate to the surrounding gas. The density and specific heat of soot are taken to be 1900 kgm^{-3} and 2100 Jkg^{-1}K^{-1} [8], respectively, while N_p and d_p are set equal to 42 and 29 nm based on the TEM study in [13]. Heat conduction in the free molecular regime is given by

$$q_{cond}\left[T_p(t)-T_g\right] = \alpha_T A_{cond}\frac{P_g c(T_g)}{8T_g}\frac{\gamma^*+1}{\gamma^*-1}\left[T_p(t)-T_g\right], \tag{4}$$

where $c(T_g) = (8k_BT_g/\pi m_g)^{1/2}$ is the mean speed of gas molecules incident on the particle surface and γ^* is an average adiabatic constant defined as [14]

$$\frac{1}{\gamma^*-1} = \frac{1}{T_p-T_g}\int_{T_g}^{T_p}\frac{d\gamma}{\gamma-1}. \tag{5}$$

Pressure and temperature are assumed to be 101.3 kPa and 300 K. The effective heat transfer area of the soot aggregate is $A_{cond} = \pi d_p^2(N_p/1.10)^{1.08}$ [15], which accounts for the greater accessibility of primary particles on the aggregate periphery to incident gas molecules compared to those within the interior of the aggregate.

The particle temperature decay rate is found by first defining $\theta(t) = T_p(t) - T_g$ and then solving Eqs. (3) and (5) to get $\ln\theta(t) = -\alpha_T C_1 t + C_2$, where

$$C_1 = \frac{3}{4}\frac{A_{cond}}{\rho_s c_s N_p \pi d_p^3}\frac{P_g c(T_g)}{T_g}\frac{\gamma^* + 1}{\gamma^* - 1}, \qquad (6)$$

and C_2 is a constant of integration. The thermal accommodation coefficient is obtained by recasting the pyrometrically-measured effective temperature in terms of $\ln[\theta(t)]$ and then performing a linear regression on the data with respect to cooling time.

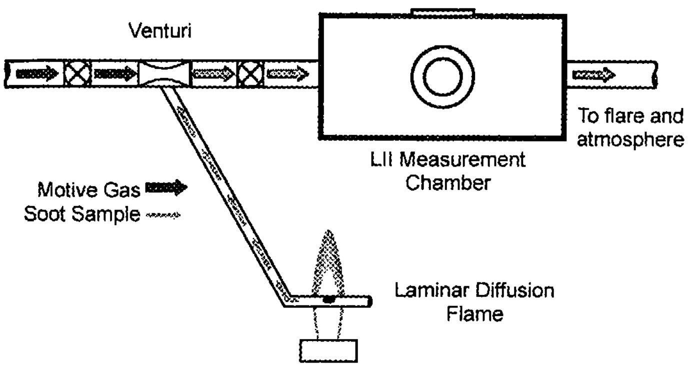

Fig. 1: Experimental apparatus.

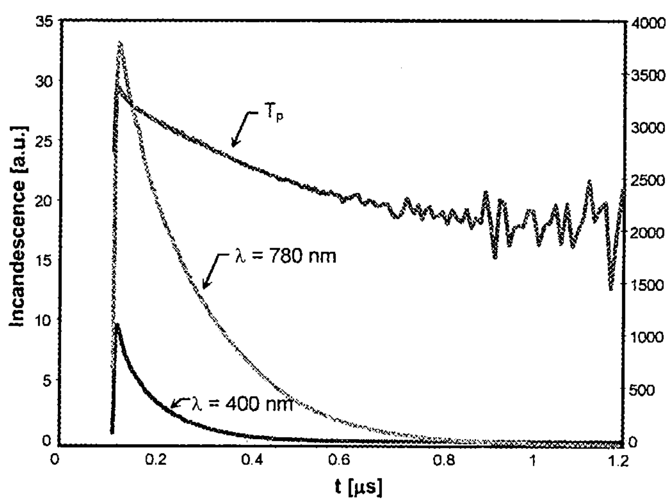

Fig. 2: LII data for soot entrained in argon.

This procedure is complicated by the fact that the observed LII signal at any instant is due to the integrated incandescence of different-sized particles cooling at rates proportional to their specific surface area. Provided the laser field is spatially uniform particles of all sizes initially cool at the same exponential rate, but at longer cooling times the pyrometric temperature decay becomes progressively non-exponential due to the non-uniform cooling of different-sized particles. There is also a commonly-observed and as yet unexplained "anomalous" cooling rate lasting 10-25 ns after the laser pulse that is particularly pronounced in LII experiments on aerosols at ambient temperatures. To address both these issues, the linear interpolation is carried out using data sampled from 50-100 ns after the peak soot temperature as shown in Fig. 3.

Thermal accommodation coefficients between soot and various gases are plotted in Fig. 4 as a function of gas molecular mass. Two main trends in the data are clearly discernable: first, α_T increases monotonically with increasing molecular mass for monatomic gases, and second, α_T becomes smaller with increasing structural complexity of the gas molecule.

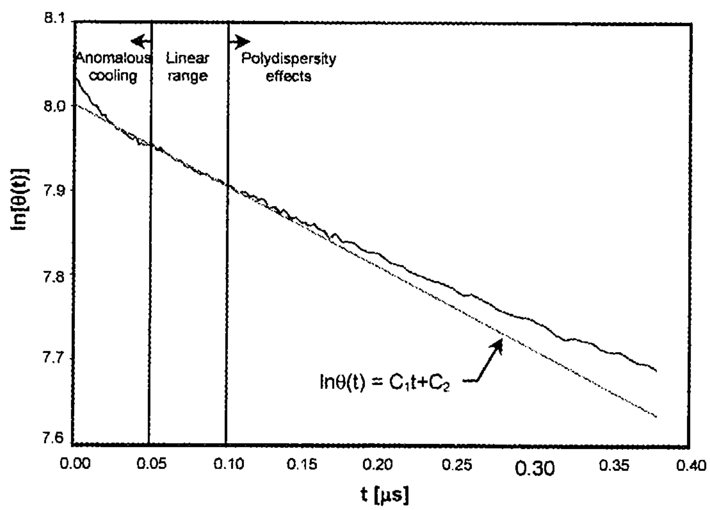

Fig. 3: Linear regression of pyrometric soot temperature measurements.

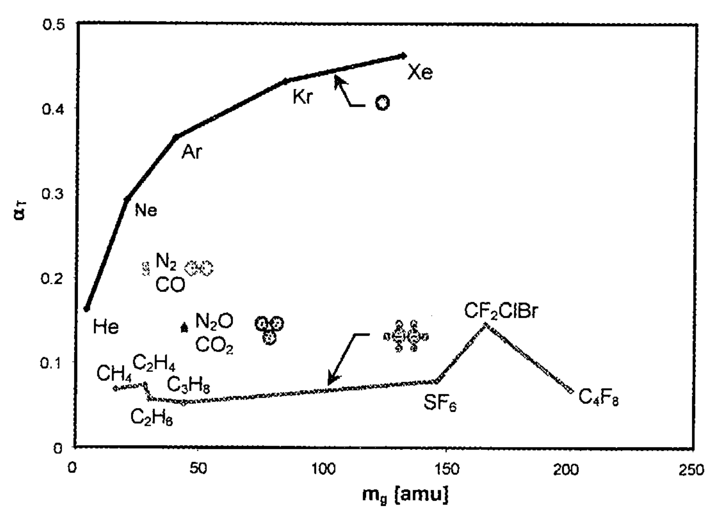

Fig. 4: Thermal accommodation coefficients versus gas molecular mass.

THERMAL ACCOMMODATION COEFFICIENTS FOR SOOT AND MONATOMIC GASES

The functional dependence of α_T on m_g for the monatomic gases can be explained by modeling gas-surface scattering as a collision between a rigid sphere and an elastic continuum surface having a density, ρ_s, Young's modulus, E_s, and Poisson ratio ν_s, and to then use continuum mechanics to calculate the deformation work done by the gas atom on the surface. From this a coefficient of restitution, e, is derived, which leads directly to α_T. Continuum mechanics was first applied to model gas-surface scattering by Landau [17], who considered one-dimensional wave propagation through the surface, and was later extended to three-dimensions by Gibley [18] and Trilling [19].

The continuum model used in this study is shown schematically in Fig. 5. To simplify the analysis, we assume a hard-sphere, normal collision between the gas molecule and the surface. If the gas molecule has approach and recoil speeds of $u_{g,i}$ and $u_{g,o}$ in the z-direction and surface has a speed V_s representative of its temperature in the positive z-direction, the thermal accommodation coefficient is

$$\alpha_T = \frac{E_o - E_i}{E_s - E_i} = \frac{(1+e)^2 + 2e\,(1+e)u_i^* + \left(e^2 - 1\right)u_i^{*\,2}}{4\left(1+u_i^*\right)}, \qquad (7)$$

where $u_i^* = u_{g,i}/V_s$, e is the coefficient of restitution,

$$e = \frac{u_{g,o} - V_s}{u_{g,i} + V_s}, \qquad (8)$$

and E_s is interpreted as the maximum outgoing kinetic energy that can be obtained by a retreating gas molecule, which occurs when $e = 1$. Note that the oscillating surface is the inertial reference frame.

The coefficient of restitution is found from the analysis of Reed [20], who applied the Hertz equations to calculate the force acting on a sphere impacting and deforming a massive elastic surface. In this case the coefficient of restitution is given by $e = (1-\Lambda)^{1/2}$, where Λ represents the fraction of incident kinetic energy transformed into deformation work over the collision duration,

$$\Lambda = 7.267\frac{\chi(\nu_s)}{\rho_s c^3}(1+\nu_s)\left(\frac{1+\nu_s^2}{1-2\nu_s}\right)^{1/2}\rho_g^{-1/5} \left[\frac{4}{3}\frac{E_s}{\left(1+\nu_s^2\right)}\right]^{6/5}\left(u_{g,i}+V_s\right)^{3/5}, \qquad (9)$$

with $c = (E_s/\rho_s)^{1/2}$ and $\chi(\nu_s)$ is a transcendental integral involving ν_s. In this analysis the Poisson ratio is set equal to 0.25 and the surface density was chosen to be 1900 kg/m^3, typical for graphitic soot [8], while V_s and E_s are left as fitting parameters. The incident gas molecule speed is the average normal velocity component of gas molecules effusing from a gas at T_g, $u_{g,i} = (\pi k_B T_g/2m_g)^{1/2}$. Equation (9) also requires an effective gas molecule density, ρ_g, which arises from the ratio of the gas molecule inertia and the area of contact between the gas molecule and the deformed surface. We set this term equal to $6m_g/\pi d_g^3$ where d_g is the hard sphere molecular diameter [21]; although this *ad hoc* procedure may seem dubious, a close examination of Eq. (9) shows that λ is much more sensitive to m_g through $u_{g,i}$ instead of ρ_g so an order-of-magnitude estimate of an effective ρ_g is sufficient for our purposes.

The effective surface velocity, V_s, and modulus of elasticity, E_s, are found by least-squares fitting Eq. (7) to the experimental results. If all data points are included in the fit, the optimum values are $V_s = 2798$ ms^{-1} and $E_s = 1.62 \times 10^{13}$ Pa, resulting in the curve shown in Fig. 6. A better fit is obtained by removing the thermal accommodation coefficient between helium and soot, which is justifiable since in this case the gas molecule can be repulsed by a solitary surface atom. Carrying out the least-squares fit without $\alpha_{T,He}$ results in $V_s = 1058$ ms^{-1} and $E_s = 3.35\times10^{12}$ Pa, giving much better overall agreement with the experimental data. For comparison, the average speed of an oscillating carbon atom is approximately $(k_B T_s/2m_g)^{1/2} \approx$ 1000 ms^{-1}. Cohen [22] shows that the covalent bonds between neighboring carbon atoms in a graphite sheet can be modeled as harmonic oscillators with a spring constant of 44.44 eV·Å^{-2}; dividing by the C-C bond length of 1.42 Å gives an estimate of the in-plane modulus of elasticity of 5.01×10^{12} Pa, which is in excellent agreement with the value obtained by least-squares fitting.

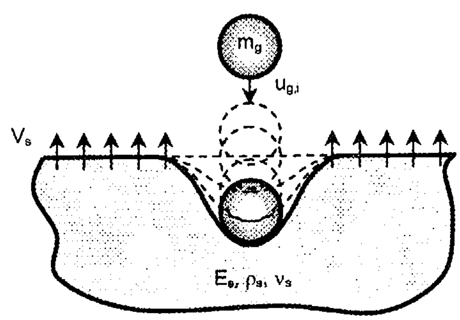

Fig. 5: Continuum model used to estimate α_T.

Equation (9) shows that α_T and λ depend on m_g primarily through the incident gas velocity, $u_{g,i}$, and not by the incident inertia of the gas molecule, $m_g u_{g,i}$, as one may intuitively expect. A gas molecule striking the surface with a high incident speed causes rapid surface deformation, requiring the gas atom to do substantial deformation work on the surface that deducts from the energy transferred from the vibrating surface to the gas atom. In a slow collision, on the other hand, the surface is more compliant since the surface atoms can move in phase with the gas molecule and relatively little collision energy is lost to deformation work. Consequently, as m_g increases $u_{g,i}$ decreases resulting in more efficient energy transfer between the vibrating surface atoms and the gas molecule, and a larger value of α_T. This mechanism has also been hypothesized by other researchers [18, 19, 23], although they predict that α_T decreases as m_g increases, since their studies take place in a regime where deformation work done by the gas molecule on the surface far exceeds thermal work done by the surface on the gas molecule. (In fact, many of these studies assume $T_s = 0$.)

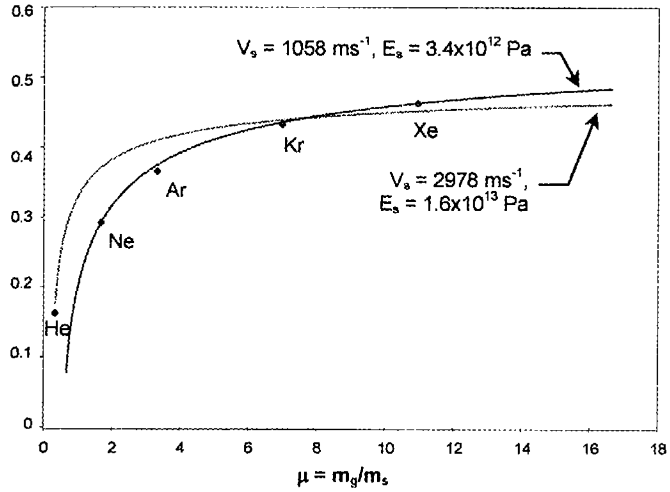

Fig. 6: Thermal accommodation coefficients derived from continuum theory.

THERMAL ACCOMMODATION COEFFICIENTS FOR SOOT AND POLYATOMIC GASES

In addition to possessing translational energy, polyatomic gases also have rotational and vibrational energy, collectively referred to as internal energy. (Electronic energy rarely plays a role in gas-surface scattering, and is neglected in this discussion.) Many LII studies implicitly assume that energy from a thermally-vibrating surface is transferred to the translational and internal modes of the gas molecules with equal efficiency, but Fig. 4 demonstrates that this is not the case since α_T is lower for more structurally-complex molecules. To account for this effect, Knudsen [24] defined separate thermal accommodation coefficients for translational and internal energy modes

$$\alpha_{T,trans} = \frac{E_{trans,o} - E_{trans,i}}{E_{trans,s} - E_{trans,i}}, \quad \alpha_{T,int} = \frac{E_{int,o} - E_{int,i}}{E_{int,s} - E_{int,i}} \quad (10)$$

based on the fact that a Maxwellian molecular steam at kinetic temperature T advects $E_{trans} = 2k_BT$ of translational energy and $E_{int} = 2/3\zeta_{int}(T)k_BT$ of internal energy per molecule. (The terms $E_{trans,s}$ and $E_{int,s}$ are the translational and internal energy per molecule carried by a molecular stream at T_s, and represent an approximate limiting case for perfect thermal accommodation, although this is strictly not the case [25].) The number of active internal energy modes, $\zeta_{int}(T)$, is obtained from

$$\zeta_{int} = \frac{5 - 3\gamma(T)}{\gamma(T) - 1}. \quad (11)$$

where the specific heat ratio is expressed as a polynomial function of temperature [26, 27]. According to Eq. (10), the thermal accommodation coefficient for internal energy is found directly from $E_{int,o}$,

$$\begin{aligned} E_{int,o} &= E_o - E_{trans,o} \\ &= \alpha_T(E_s - E_i) + E_i \\ &\quad - \left[\alpha_{T,trans}\left(E_{trans,s} - E_{trans,i}\right) + E_{trans,i}\right], \end{aligned} \quad (12)$$

provided that $\alpha_{T,trans}$ is also known. Based on the assumption that $\alpha_{T,trans}$ depends only on m_g through $u_{g,i}$ and is independent of gas molecular structure, the translational thermal accommodation coefficient for each polyatomic gas is estimated from Eq. (7-9) with V_s = 1058 ms^{-1} and E_s = 3.35×10^{12} Pa, as shown in Fig. 7.

Figure 8 shows that the values of $\alpha_{T,int}$ is substantially lower than $\alpha_{T,trans}$, and furthermore, even though the amount of internal energy generally increases with the number of active degrees of freedom, $\alpha_{T,int}$ tends to decrease with $\zeta_{int}(T_g)$. This implies that energy is preferentially accommodated from the soot surface into the rotational modes of the gas molecule instead of the vibrational modes since the latter represent a larger portion of the active internal energy modes as the molecular structure becomes more complex. This finding is consistent with the results of molecular beam scattering experiments involving SF_6/graphite [28] and CF_3Br/graphite [29] and is not surprising given the long relaxation times of vibrational energy modes [30, 31], although further molecular dynamics studies are needed to show how exactly the collision mechanics influence vibrational accommodation.

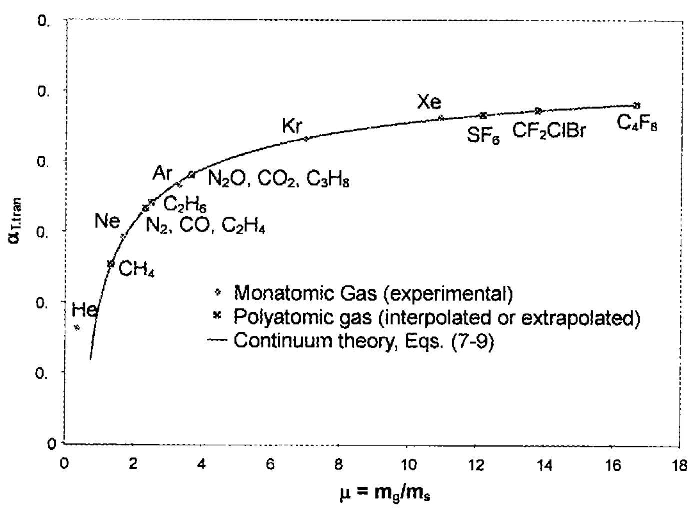

Fig. 7: Translational thermal accommodation coefficients are found by interpolating and extrapolating from the monatomic gas dataset.

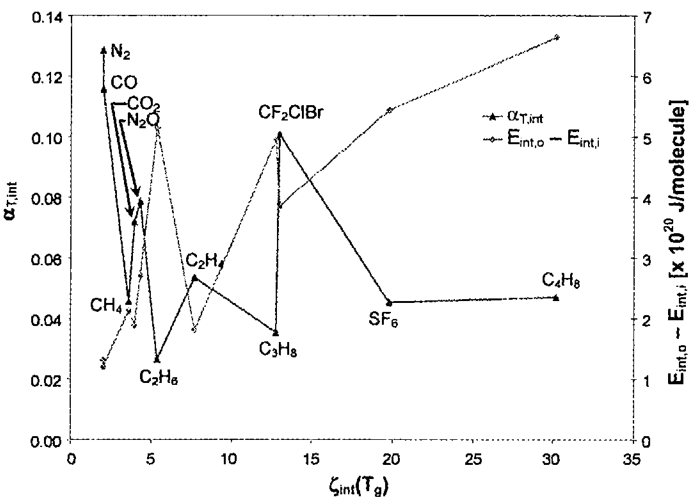

Fig. 8: Internal thermal accommodation coefficients and net energy transfer between soot and polyatomic gas molecules.

CONCLUSIONS

Understanding the fundamental physics of gas-surface scattering is crucial when using time-resolved laser-induced incandescence to measure the particle size distribution in aerosols. This paper endeavors to explore this physics using experimentally-measured accommodation coefficients between soot and various monatomic and polyatomic gases

In general, the thermal accommodation coefficient of monatomic gases increases with the molecular mass of the gas. A simple model based on continuum mechanics suggests that α_T is a function of the molecular mass of the gas through impact speed and rate of surface deformation. Collisions involving heavier, slower-moving gas molecules are characterized by higher coefficients of restitution, and consequently more collision energy is transferred to the outgoing kinetic energy of the gas molecule.

A comparison of the thermal accommodation coefficients between monatomic and polyatomic gas molecules reveals that the energy is transferred preferentially to the translational energy mode of the gas molecule over the rotational and vibrational modes. The internal energy accommodation coefficient decreases as the number of internal degrees of freedom increases because energy is transferred preferentially to rotational energy modes rather than vibrational modes.

We are presently developing a molecular dynamics simulation to validate the results of our simplified continuum-mechanics model. The relationship between translational thermal accommodation and incident gas velocity shall also be confirmed experimentally by measuring the thermal accommodation coefficient between soot and a monatomic gas at various gas temperatures. Finally, an in-depth comparison of molecular structure to the experimental results and further molecular dynamics simulation will clarify the accommodation of rotational and vibrational energy modes.

ACKNOWLEDGMENTS

The authors are grateful to Mr. Reg Smith, Mr. Bob Sawchuk, and Mr. Dan Clavel for their assistance in conducting the experiments, and Dr. Barry Stagg for suggesting the sampling apparatus.

REFERENCES

[1] Knudsen, M., 1911, "Die Molekulare Wärmeleitung der Gase und der Akkommodationskoeffizient,"Ann. Physik, **339**, 4, pp. 593-656.

[2] Daun, K. J., Stagg, B. J., Liu, F., Smallwood, G. J., and Snelling, D. R., 2007, "Determining Aerosol Particle Size Distributions using Time-Resolved Laser-Induced Incandescence" Applied Physics B, in press, DOI i10.1007/s00340-007-2585-y.

[3] Goodman, F. O., and Wachman, H. Y., 1976, Dynamics of Gas-Surface Scattering, Academic Press, New York, NY, pp. 257-268.

[4] Saxena, S. C., and Joshi, R. K., 1981, Thermal Accommodation and Adsorption Coefficients of Gases, McGraw-Hill, New York, NY, pp. 61-131.

[5] Lehre, T., Jungfleisch, B., Suntz, R., and Bockhorn, H., 2003, "Size Distributions of Nanoscaled Particles and Gas Temperatures from Time-Resolved Laser-Induced-Incandescence Measurements," Applied Optics, **42**, 12, pp. 2021-2029.

[6] Starke, R., Kock, B., and Roth, P., 2003, "Nano-particle Sizing by Laser-Induced-Incandescence (LII) in a Shock Wave Reactor," Shock Waves, **12**, 351-360.

[7] Kuhlmann, S.-A., Schumacher, J., Reimann, J., and Will, S., 2004, "Evaluation and Improvement of Laser-Induced Incandescence for Nanoparticle Sizing," Proc. PARTEC 2004, Nuremberg, March 16-18, 2004.

[8] Snelling, D. R., Liu, F., Smallwood, G. J., and Gülder, Ö. L., 2004, "Determination of the Soot Absorption Function and Thermal Accommodation Coefficient using Low-Fluence LII in a Laminar Co-flow Ethylene Diffusion Flame," Combustion and Flame, **136**, pp. 180-190.

[9] Eremin, A. V., Gurentsov, E. V., Hofmann, M., Kock, B. F., and Schulz, C., 2006, "TR-LII for Sizing of Carbon Particles Forming at Room Temperature," Applied Physics B, **83**, 3, pp. 449-454.

[10] Liu, F., Snelling, D. R., and Smallwood, G. J., 2005, "A Critical Evaluation of the Thermal Accommodation Coefficient of Soot Determined by the Laser-Induced Incandescence

Technique," Proc. International Bunsen Discussion Meeting 2005, Duisburg, Germany, Sep. 25-28, 2005.

[11] Schulz, C. Kock, B. F., Hoffman, M., Michelsen, H., Will, S., Bougie, B., Suntz, R., and Smallwood, G., 2006, "Laser-Induced Incandescence: Recent Trends and Current Questions," Applied Physics B, **83**, pp. 333-354.

[12] Snelling, D. R., Thomson, K. A., Smallwood, G. J., and Gülder, Ö. L., 1999, "Two-Dimensional Imaging of Soot Volume Fraction in Laminar Diffusion Flames," Applied Optics, **38**, 12, pp. 2478-2485.

[13] Tian, K., Thomson, K. A., Snelling, D. R., Smallwood, G. J., and Wang, D. S., 2004, "Distribution of the Number of Primary Particles of Soot Aggregates in a Nonpremixed Laminar Diffusion Flame," Combustion and Flame, **138**, 1-2, pp. 195-198.

[14] Filippov, A. V., and Rosner, D. E., 2000, "Energy Transfer between an Aerosol Particle and Gas at High Temperature Ratios in the Knudsen Regime," IJHMT, **43**, 1, pp. 127-138.

[15] Brasil, A. M., Farias, T. L., and Carvalho, M. G., 1999, "A Recipe for Image Characterization of Fractal-like Aggregates," J. Aerosol Sci., **30**, 10, pp 1379-1389.

[16] Goodman, F. O., and Wachman, H. Y., 1976, Dynamics of Gas-Surface Scattering, Academic Press, New York, NY, pp. 306.

[17] Landau, L., 1935, "On the Theory of the Accommodation Coefficient," Physikalische Zeitschrift der Sowjetunion, **8**, pp. 489., as reported in [4].

[18] Gibley, D. M., 1962, "A Re-examination of Thermal Accommodation Coefficient Theory," J. Phys. Chem. Solids, **23**, pp. 1453-1461.

[19] Trilling, L., 1970, "The Interaction of Monatomic Inert Gas Molecules with a Continuous Elastic Solid," Surface Science, **21**, pp. 337-365.

[20] Reed, J., 1985, "Energy Losses due to Elastic Wave Propagation during an Elastic Impact," Journal of Physics D, **18**, pp. 2329-2337.

[21] Bird, G. A., 1994, Molecular Gas Dynamics and the Direct Simulation of Gas Flows, Oxford Science Publications, Oxford, UK, pp. 409.

[22] Cohen, L. K., 1993, "A Lower Bound on the Loss of Grapite by Atomic Oxygen Attach at Asymptotic Energy," J. Chem. Phys, **99**, 12, pp. 9652-9663.

[23] Goodman, F. O., 1962, "The dynamics of simple cubic lattices II: The effects of surface impurities on the lattice motion," Journal of Physics and Chemistry of Solids, **23**, 11, pp. 1491-1502.

[24] Knudsen, M., 1930, "Radiometerdruck und Akkommodationskoeffizient," Ann. Physik, **398**, 2, pp. 129-185.

[25] Goodman, F. O., and Wachman, H. Y., 1974, "Restrictions on the Values of Energy Accommodation Coefficients," Surface Science, **43**, pp. 306-308.

[26] McBride, B. J., Gordon, S., and Reno, M. A., 1993, "Coefficients for Caculating Thermodynamic and Transport Properties of Individual Species," NASA Technical Memorandum 4513.

[27] Burcat, A., and Ruscic, B., 2005, "Third Millennium Ideal Gas and Condensed Phase Thermochemical Database for Combustion with updates from Active Thermochemical Tables," Argonne National Laboratory Report ANL-05/20 and Technion Report TAE 960.

[28] Andersson, M. B., and Pettersson, J. B. C., 1996, "Vibrational Excitation of SF_6 Scattering from Graphite," Chemical Physics Letters, **250**, pp. 555-559.

[29] Andersson, M. B., Pettersson, J. B. C., and Marković, N., 1997, "Vibrational Excitation of CF_3Br Scattering from Graphite," Surface Science, **384** , L880-L885.

[30] Patterson, G. N., 1956, Molecular Flow of Gases, John Wiley, New York, NY, pp. 145.

[31] Levine, R. D., and Bernstein, R. B., 1987, Molecular Reaction Dynamics and Chemical Reactivity, Oxford University Press, Oxford, UK, pp. 312-315.